An evaluation of void filling interpolation methods for SRTM data

H. I. REUTER*§, A. NELSON† and A. JARVIS‡

§ Institute for Environment and Sustainability – Land Management and Natural Hazards Unit, European Commission - DG Joint Research Centre, TP 280, Via Fermi 1, I - 21020 Ispra (VA) Italy,

hannes.reuter@jrc.it, Tel: 39-0332-785535, Fax: 39-0332-786394

†Institute for Environment and Sustainability – Global Environment Monitoring Unit, European Commission - DG Joint Research Centre, TP 440, Via Fermi 1, I - 21020 Ispra (VA) Italy,

andrew.nelson@jrc.it, Tel: 39-0332-786744, Fax: 39-0332-789073

‡International Center for Tropical Agriculture (CIAT) and International Plant Genetic Resources Institute (IPGRI), Recta Cali-Palmira, km 17, AA6713 Cali, Valle del Cauca, Colombia,

a.jarvis@cgiar.org, Tel: 57-2-4453265, Fax: 57-2-4450073

* Corresponding author: Hannes Isaak Reuter Email: hannes.reuter@jrc.it, Tel: 39-0332-785535, Fax: 39-0332-786394

ABSTRACT

The Digital Elevation Model that has been derived from the February 2000 Shuttle Radar Topography Mission (SRTM) has been one of the most important publicly available new spatial datasets in recent years. However, the 'finished' grade version of the data (also referred to as Version 2) still contains data voids (some 836,000 km^2) – and other anomalies – that prevent immediate use in many applications. These voids can be filled using a range of interpolation algorithms in conjunction with other sources of elevation data, but there is little guidance on the most appropriate void filling method. This paper describes: (i) a method to fill voids using a variety of interpolators, (ii) a method to determine the most appropriate void filling algorithms using a classification of the voids based on their size and a typology of their surrounding terrain; and (iii) the classification of the most appropriate algorithm for each of the 3,339,913 voids in the SRTM data. Based on a sample of 1,304 artificial but realistic voids across six terrain types and eight void size classes, we found that the choice of void filling algorithm is dependent on both the size and terrain type of the void. Contrary to some previous findings, the best methods can be generalised as: Kriging or Inverse Distance Weighting interpolation for small and medium size voids in relatively flat low-lying areas; Spline interpolation for small and medium sized voids in high altitude and dissected terrain; Triangular Irregular Network or Inverse Distance Weighting interpolation for large voids in very flat areas, and an advanced Spline Method (ANUDEM) for large voids in other terrains.

Key words: DEM, interpolation methods, void filling, DEM fusion

1. Introduction

A Digital Elevation Model (DEM, or more correctly a Land Surface Model - LSM) is one of the most useful sources of information for spatial modelling and monitoring, with applications as diverse as: Environment and Earth Science, e.g. catchment dynamics and the prediction of soil properties; Engineering, e.g. highway construction and wind turbine location optimisation; Military, e.g. land surface visualisation, and; Entertainment, e.g. landscape simulation in computer games (Hengl and Evans 2007). The extraction of land surface parameters – whether they are based on 'bare earth' models such as DEMs derived from contour lines and spot heights, or 'surface cover' models derived from remote sensing sources that include tree top canopies and buildings for example – is becoming more common and more attractive due to the increasing availability of high quality and high resolution DEM data (Gamache 2004). One of the most widely used DEM data sources is the elevation information provided by the Shuttle Radar Topography Mission (SRTM) (Coltelli *et al.* 1996, Farr and Kobrick 2000, Gamache 2004), but as with most other DEM sources, the SRTM data requires significant levels of pre-processing to ensure that there are no spurious artefacts in the data that would cause problems in later analysis such as pits, spikes and patches of no data (Dowding *et al.* 2004, Gamache 2004, Chaplot *et al.* 2006, Fisher and Tate 2006). In the case of the SRTM data, these patches of no data are pervasive (USGS 2006b) and must be filled or interpolated, preferably with auxiliary sources of DEM data. This paper describes a procedure to determine the most appropriate interpolation methods (with and without auxiliary DEM data) for no data patches of different sizes and in different terrain types. The rationale for this paper stems from a statement by Fisher and Tate (2006) that no single interpolation method exists for the most accurate interpolation of terrain data. Such a procedure is necessary for developing a high quality global DEM derived from the SRTM data where all no data areas have been filled using the best performing interpolation algorithm available.

1.1. *The Shuttle Radar Topography Mission (SRTM)*

The 11 day Shuttle Radar Topography Mission (SRTM) flew in February 2000, and has provided publicly available elevation surface data for approximately 80% of the world's land surface area (from 60ºN to 56ºS), with a post spacing of 1 arc seconds (often quoted as 30 metres resolution) in the USA, and a degraded 3 arc second (often quoted as 90 metres resolution) product for the rest of the world. It is a snapshoot of the reflective surface of the earth during the time period of the mission, and is about 100 times more detailed than other existing freely available global elevation data, such as GTOPO30 (USGS 1996) and GLOBE (Hastings and Dunbar 1998). The SRTM elevation data is derived from X-band and C-band Interferometric Synthetic Aperture Radar (InSAR) (Werner 2001, USGS 2006b). This paper deals with the better known and widely available C-band product, which we will refer to as SRTM elevation data. As with all DEMs derived from remote sensing sources, the SRTM elevation data include trees, buildings and other objects on the earth surface and therefore the dataset is a surface elevation model (Rodriguez *et al.* 2005, 2006).

Several products have been derived from the SRTM data. Firstly, the raw data was processed by a suite of programs at JPL (Farr and Kobrick, 2000), and was made available primarily for research purposes. This was termed "unfinished" data. Further processing generated DEMs in full DTED compliance level, and these were termed "finished" data (Slater *et al.*, 2006). For both datasets: elevations outside the USA are degraded either by (i) averaging or (ii) by thinning (i.e. taking one sample out of the nine available posts). The horizontal datum of the SRTM data is WGS84, whilst the vertical datum is EGM96 which has implications for certain applications.

The C-band product has significant areas of missing data due to the nature of radar data and the interferometric process used to create the DEM (Figure 1). The reasons for the missing data are geometric artefacts, specular reflection of water, phase unwrapping artefacts and voids due to complex dielectric constant (see Kervyn 2001 for further information). For example, the InSAR instrument used to generate the SRTM elevation data had an incidence angle of between 30º and 60º, making it difficult to generate images for terrain slopes corresponding to that range of angles (Gamache 2004, Eineder 2005).

For the purpose of this paper, we define any areas of missing data that exists in the SRTM data as voids. The number of remaining voids with different sizes in the SRTM data are a considerable problem for many uses and applications, including hydrological modelling, terrain indices, land surface characterisation, digital soil mapping and many other geomorphometric models, and thus these voids need to be filled to create a seamless DEM (MacMillan *et al.* 2000).

The "finished" version of the SRTM data (described more fully in section 2.1) provided by USGS (United States Geological Survey) and NASA (National Aeronautics and Space Administration) still contains 3,399,913 voids accounting for 803,166 km^2 (an area comparable to Pakistan or somewhat larger than Texas), and in extreme cases, such as Nepal, they constitute 9.6% of the country area with some 32,688 voids totalling an area of 13,740 km^2. Figure 1 shows the proportion of each 1 × 1 degree SRTM tile that is composed of void areas. Figure 2 shows two extreme examples of regions where there are many voids, Libya (upper) and Nepal (lower). Of the 210 countries covered by the SRTM data, two countries have void areas larger than 10% of their country size, nine countries more than 5% and 14 more than 2%. In total, 44 countries have 1% or more of their area covered by voids. The void size / frequency distribution of all voids in the SRTM dataset is shown in Figure 3.

[Insert figure 1]

[Insert figure 2]

[Insert figure 3]

Voids occur for different reasons in different terrain types: a void due to shadowing will more likely occur in mountainous areas, whereas a void due to complex dielectric constant is more likely to occur in desert areas like the Sahara. Void frequency with respect to elevation has been demonstrated to have a bimodal distribution with peaks of the distribution occurring in flat areas and in steeply sloping areas (Gamache 2004, Falorni *et al.* 2005). This distribution is clearly seen in Figure 1.

Since this study focuses on methods of void filling the SRTM elevation data, we will not discuss the accuracy or the errors in the SRTM data, though it is worth mentioning that the sensor error is stated to be +/-16m (USGS, 2006b). Further details on SRTM accuracy are available in the literature (Toutin 2002, Rabus *et al.* 2003, Gamache 2004, Falorni *et al.* 2005).

Fisher and Tate (2006) provide a thorough review of the causes and consequences of error in DEMs. They classify errors into three different groups: (i) gross errors (e.g. system malfunctions), (ii) systematic errors, which might be described by a functional relationship (Thapa and Bossler, 1992: p836 in Fisher and Tate 2006), and (iii) random errors with/without spatial dependence that arise for different reasons. Voids are one type of systematic error, which can be overcome with specific algorithms.

1.2. *Void filling methods*

Interpolation methods are widely used in the generation of DEMs. However, void filling (VF) methods contain a special subset of interpolation algorithms with certain restrictions, and also other methods such as the fill and feather approach (Dowding *et al.,* 2004). All interpolation algorithms for void filling DEMs use the elevation data surrounding the void in the interpolation process. If auxiliary sources of elevation (for example, ASTER DEMs, GTOPO30, digitised topographic maps and land survey measurements) are available, then some of these algorithms can incorporate this information to improve the accuracy of the interpolation. However, there are often severe differences between the DEM and the auxiliary data that need to be addressed before the void filling algorithms can use auxiliary data. These differences can occur in : (i) the spatial resolution, (ii) the vertical datum, (iii) horizontal and vertical shifts, (iv) first or second order trends, (v) production errors, (vi) the type of Surface Model (SRTM is a surface model, whereas a DEM based on topographic data is a bare earth model) and, (vii) the spatial distribution of errors (see for example Hutchinson, 1989, Kaab 2005, Fisher and Tate 2006).

VF algorithms can be categorised into surface (Katzil and Doytsher 2000), volumetric (Vedera *et al.* 2003) or example based methods (Sharf *et al.* 2004). Alternatively, Katzil and Doytsher (2000) divide the algorithms into polynomials (such as linear estimation, 1D and 2D polynomials of the third order, cubic splines, or iterative spline algorithms) and non polynomial approaches (such as kriging, inverse distance weighting, fill and feather approaches or moving average).

Several authors have evaluated the quality of different algorithms to fill in voids for radar data as well as other DEM sources. Katzil and Doytsher (2000) tested linear estimation, kriging and cubic spline for elevation, but the evaluation was not performed on real voids. Instead a method called cross-validation was applied (removing one point and then comparing the elevation of the generated surface against the elevation of the point), which showed no significant differences between methods. Dowding *et al.* (2004) used a fill and feather (FF) approach (i.e. they used an auxiliary elevation dataset to patch the void area, and then smoothed the transition zone between both datasets) to incorporate auxiliary information into a VF algorithm. They selected seven voids with sizes ranging from 36 to 2,541 pixels and then compared the results both visually and against a reference DEM and ground control points. The results showed differences between 0 m and 22 m for the area of seven different voids against a reference DEM. Kuuskivi *et al.* (2005) used seven real world voids across different terrain types to evaluate the performance of a commercial fill and feather algorithm that used high quality auxiliary DEM data against three freeware programmes: 3DEM (Visualization Software LLC, 2004); VTBuilder (Virtual Terrain Project, 2004); and BLACKART (TerrainMap.com, 2004). The study clearly demonstrated the large differences in results that can occur when using different VF algorithms and the potential improvements that can be achieved with good quality auxiliary information. Grohman *et al.* (2006) presented a geostatistical algorithm (Inverse Distance Weighting - IDW) together with a linear adjustment of the elevation height called Delta Surface Fill (DSF) and compared it against a FF approach using five artificially created voids in void prone terrain types from the SRTM data. The authors concluded that the performance of the DSF algorithm produced better results based on visual interpretation and reduced the standard deviation of the error surface.

Several other studies have presented algorithms that are capable of filling void areas, but did not provide statistical results. For example Hofer *et al.* (2006) tested an advanced cubic spline method which keeps certain error bounds on nine voids and evaluated the void filling results graphically. Almansa *et al.* (2006) evaluated four different artificial voids at different locations by comparing three different methods. Another example is Kääb (2005) whereby a simple replacement of SRTM by ASTER data was made without any further evaluation.

There are several observations that can be drawn from these studies. Firstly, each study typically compares three or four algorithms at most, whereas a GIS may contain many more suitable algorithms (e.g. IDW, Kriging, ANUDEM, Spline, and Trend Estimation). Secondly, some of the studies contain algorithms that are not easily reproducible within a GIS or Image Analysis System because their description is too vague or due to commercial interests. We argue that if an improved global DEM is to be produced from the SRTM data, then the VF algorithms should be accessible and repeatable. Thirdly, the studies presented results based on a handful of voids which may not be representative of the 3,339,913 voids in the SRTM data, and are not sufficient for robust statistical analysis. A much larger sample of real world voids is required before we can suggest one algorithm over another with any degree of confidence. Fourthly, occasionally these voids were artificial and hence may not be representative of real world voids. We realise that unless a high quality auxiliary DEM is available, then it is impossible to assess the veracity of the results from void filling as there is no ground truth data. However, it is possible to create artificial voids that are representative of real voids in terms of size, shape and terrain location. Fifthly, terrain can have a large influence on VF results. Katzil and Doytsher (2000) acknowledged that terrain has an influence on the void filling process; however, they could not suggest a recommended method across three terrain types (mountains, hilly and planar). Grohman *et al.* (2006) recognised the relief type for their five voids, which lead to decreasing average standard deviation from rugged to moderate to flat terrain. Again, the sample of voids should be sufficiently large across a range of terrain types in order to assess the influence of terrain ruggedness on algorithm choice and performance. Finally, void size is critical. It is much harder to accurately fill a large void than a small one. Grohman *et al.* (2006) recognised the importance of void size, but did not provide further insight. Again, the sample of voids should include sufficient numbers of voids of sizes that are representative of voids found in each terrain type.

In conclusion, there has been no thorough evaluation of the many (GIS ready) VF algorithms for DEM data using a sufficient number of voids of varying size across different terrain types in order to determine the most appropriate VF method(s).

1.3. *Research objectives*

The objectives of this study are to: (i) describe void characteristics in terms of size and terrain unit; (ii) determine which VF algorithm performs best without any auxiliary information on an exhaustive dataset, with respect to terrain unit and void size; (iii) determine if low grade auxiliary information can improve the VF algorithm performance; (iv) determine which VF algorithm performs best with respect to terrain unit and void size using auxiliary information, and; (v) provide a global void dataset stating the best VF algorithm that should be used based on the results from (ii) and (iv).

2. Study area and data

As shown in Figure 1, data voids occur in all regions of the SRTM data, but after consideration of the spatial distribution of voids and terrain units and computational limitations we limited our sample of voids to Africa, an area of approximately 29,800,000 km^2 and containing 1,168,136 voids. This provided a sufficient number of voids across a wide range of sizes and terrain units from which to perform the sampling.

2.1. SRTM data preparation

SRTM data is available in different formats from different distributors (a testament to its usefulness and popularity), and here we use the "finished" 3-arc second averaged SRTM data set that is available from the USGS EROS data server (USGS 2006a). The pre-processing and editing of this data is described in (USGS 2006b), but the essential details are that spikes and pits in the data with surrounding elevation differences greater than 100 m were removed, voids smaller then 16 pixels were filled with a nearest neighbour interpolation while larger voids were left as were, and water bodies and coastlines were depicted as described in (USGS 2006c). The data are available in one × one degree tiles in 16 bit integer BIL format. 3,250 tiles were downloaded from ftp://e0srp01u.ecs.nasa.gov/srtm/version2/SRTM3/Africa and were converted to

ESRI™ grid format and mosaicked together in ArcGIS 9.1© to create a continental DEM for Africa with extents 39ºN-35ºS and 30ºW-60ºE. Since this data has been edited for small voids, coastlines and water bodies, we assume than any remaining land area which contains no elevation information is a void.

For each of the 1,168,136 voids we stratified the voids based on the natural logarithm of the number of void pixels and grouped them into eight size classes with the following number of pixels (numbers in parentheses are minimum, average and maximum) per class; [A] (1,10,25), [B] (26,50,80), [C] (81,120,140), [D] (141,240,400) [E] (401,600,800) [F] (801,1100,2500), [G] (2501,4000,8000) and [H] (8001,10000,1267052).

2.2 Auxiliary DEM data

As stated in section 1.2, some VF methods incorporate auxiliary DEM information in order to improve the accuracy of the results. In this study we used the SRTM30 (Gamache 2004, USGS 2006d) and GTOPO30 DEMs (see sections 1.1 and 2.1 for more details on these two datasets), which were stored in ESRI™ grid format, as these are the only DEM datasets available for all of Africa.

2.3 Terrain typology

The terrain typology is based on the SRTM30 data. A half degree resolution, 15 class terrain typology was derived from this DEM based on a combination of the average SRTM30 elevation within each half degree pixel and the relief roughness of the SRTM30 data within the pixel, defined as the range of SRTM30 elevation values in the pixel divided by half the pixel length connecting the centre of each grid pixel (Meybeck *et al.* 2001). For simplification, we aggregated these 15 classes into six major terrain units (TU), which have similar land surface characteristics. The relief classes (1) plains, (2) mid-altitude plains and (3) high-altitude plains were grouped into PLAINS; (4) lowlands, (6) platforms, (7) low plateaus, and (8) mid-altitude plateaus were grouped into PLATEAUS; (9) high plateaus and (10) very high plateaus were grouped into HIGH PLATEAUS; (5) rugged lowlands and (11) hills were grouped into HILLS, (12) low mountains, (13) mid altitude mountains were grouped into MOUNTAINS, and; (14) high mountains, and (15) very high mountains were grouped into HIGH MOUNTAINS. Figure 4 shows the original 15 terrain classes for Africa and their grouping into six major terrain units .

The sizes of terrain units are quite different across Africa. Void size is also significantly different between TU. Therefore we used that as additional stratification factor, which allowed us to assess differences between TU (Fig 5). The highest percentage of void area per total TU area is reached in PLAINS, which can be attributed to the dunes in desert areas, followed by voids in HIGH MOUNTAINS. The PLAINS cover between 30- 50% of all large void areas (void size groups G and H), with a percentage around 20 % for all other size classes. HIGH MOUNTAINS on the other hand covers shows an increase from 20% to 30% over all size classes (except the H size class). A decreasing percentage of voids can be observed for PLATEAUS, MOUNTAINS and HILLS with increasing void size, whereas the HIGH PLATEAUS show a strong increase in percentage of voids with increasing size class (Fig. 5).

[Insert Figure 4]

[Insert Figure 5]

2.4 *Void selection*

The voids were sampled using the following procedure. We first identified the terrain unit of each of the 1,168,136 voids. For the few occasions where a void lay in the boundary between two terrain units, it was assigned to the terrain unit in which the greater area of the void lay. No TU was assigned in the very few cases where a void was evenly distributed over two or more terrain units. In the cases where the half degree resolution TU map did not extend over coastal voids the closest TU pixel (almost always PLAINS) was assigned to the void. Secondly, the previously discussed size class was assigned to each void. The distribution of all the voids by terrain unit and size class is shown in Table 1. The distribution by terrain units agrees with the findings of Falorni *et al.* (2005), but we have found no corresponding study for the distribution of void sizes and void size by terrain unit.

[Insert Table 1]

Within each terrain unit we randomly selected 15 voids based on their size distribution (i.e. we selected more small voids than large ones in a given terrain unit if small voids occurred more frequently). We then duplicated each of these voids a number of times, again in relation to their size distribution, and manually relocated them to neighbouring locations within the same terrain unit, ensuring that the void was relocated to a similar landscape and that it did not overlap with existing voids. For example, a small void (size class A) in terrain unit PLAIN would be duplicated 15 times and moved to 15 neighbouring locations in terrain unit PLAIN to create 15 voids for analysis. Duplication of real void areas ensures that the shape, size and orientation of the artificial voids are representative of real voids. However, it does risk the creation of artificial voids in areas of the terrain that are not representative of the terrain of the real void. To ensure that we relocated the voids to comparable terrain, we employed (i) visual inspection of the terrain and (ii) computed the mean and standard deviation of the elevation in a buffer zone surrounding the real void and compared it the mean and standard deviation of the elevation in buffer zones surrounding the relocated void. No significant changes could be observed in the standard deviation of the surrounding elevation between the groups of relocated and the real voids across the original 15 terrain types (based on a *t* test), except for rugged lowlands and low plateaus. No differences were observed when the results were aggregated into the six terrain units (results not shown). Therefore we assume that the visual relocation was an acceptable approach for generating realistic artificial voids.

In this way we created 1,304 artificial but realistic voids based on real void characteristics distributed across six terrain units and eight size classes (Table 2). These voids were stored as polygon coverages in ArcInfo.

[Insert Table 2]

2.5 Data pre-processing for the artificial voids

A working area for each single void was created by enlarging the maximum extent of the void by 100 pixels in all directions and extracting the underlying DEM data within this buffer zone. The number of pixels for this buffer was based on empirical testing of the algorithm under different terrain units (results not shown). We then ‘punched out’ the void from this buffered area and used the remaining ‘ring’ of DEM data to create (i) elevation spot heights or points, with one point for each DEM pixel, and, (ii) contours at 10 m intervals. There were occasions where it was not possible to extract contours from the buffered region, for example where the terrain was extremely flat. In these cases we employed an iterative process to decrease the contour interval until a contour layer could be created (the lower limit was 1 m). Where this process did not result in a contour layer, we extended the buffer up to a maximum threshold of 0.1 degrees. These contours were stored as line or point coverages in ArcInfo.

Auxiliary spot height elevation data was extracted from the SRTM30 and GTOPO30 at 30 arc second spacing unless either one of two restrictions were met. The first restriction is the size of the void (coarse auxiliary data will not help in the interpolation of small voids); and the second considered the shape of the void (e.g. a long, thin void is better filled with only the surrounding DEM data).

SRTM data have a high absolute accuracy in contrast to GTOPO30 and to account for such differences we adjusted the elevation values in the GTOPO30 DEM as follows. For each void, the auxiliary DEM was re-sampled to the resolution of the SRTM dataset and the void area was punched out from this re-sampled auxiliary dataset. The difference in elevation between both datasets was used to raise or lower the elevation values for the original resolution auxiliary dataset. Thereby we accounted for some differences between datasets (i, ii, vii) as outlined in section 1.2. We did not make any adjustments for other errors (e.g. geometrical location or trends in the auxiliary data). The spot heights were stored as point coverages in ArcInfo.

The SRTM elevation from the void stamped area constitutes the ‘truth’ layer against which the results from the VF algorithms were compared. Essentially, this is equivalent to withholding pixels from the interpolation process and then comparing the results from the VF algorithms against them afterwards (see also Yang and Hodler, 2000).

Thus, for each of the 1,304 voids we created a truth DEM, a set of contours and spot heights buffering an artificial void area, and where applicable, two auxiliary spot height datasets.

3. Void filling methods

The procedure for applying and evaluating the VF algorithms is outlined in Figure 6 and described in detail in the following sections. Unless otherwise stated, all processing was carried out in ArcInfo Workstation 9.1 using Arc Macro Language (AML) routines and standard ArcInfo interpolation functions from the Arc and Grid environments. The results of the VF methods were projected from geographic projection (latitude/longitude) into Mollweide Equal Area projection where the longitude of the projection centre was the longitude of the centroid of the void, and both vertical and horizontal units were in metres.

[Insert Figure 6]

3.1 Void filling methods

The following eight VF algorithms were implemented:

i) Kriging (KR), ii) Spline (SP), iii) Trend (TR), iv) Inverse Distance Weighting (IDW), v) Moving Window Average (MW), vi) Fill and Feather (FF), vii) Triangulated Irregular Network (TIN) and viii) ANUDEM (ANU).

The geostatistical methods (KR, SP, TR and IDW) require several input parameters, but we used default values wherever possible, since it was too complex and too time consuming to adjust the parameters for each method and each void. One might criticise this approach since adjusting the parameters could improve the interpolations on a case by case basis. However since the VF algorithms are all well known and long standing implementations, we assume that the default values provide reasonable results under most conditions.

The implementation for KR is based on McBratney *et al.* (1986), using a spherical semi-variogram model with an automatically fitted function. We used a 10th order linear polynomial regression (based on manual testing, results not shown) for TR. The SP method follows Franke (1982) and Mitas and Mitasova (1988) and performs a two-dimensional minimum curvature spline interpolation resulting in a smooth surface that passes exactly through the input points. In this case we used regularised splines which yield a smooth surface. We did not test tension splines as in Mitasova and Hofierka (1993), even though it is available as an option in ArcInfo. IDW was implemented following Watson and Philip (1985) based on the 12 nearest neighbouring points.

MW interpolates the void area by computing elevation values in the void pixels next to the void boundary based on the local average of the neighbouring elevation pixels. This process continues inwards until all void pixels are filled. For FF, we re-sampled the auxiliary information to the resolution of the truth DEM, buffered it inwards, filled in the void using this re-sampled auxiliary DEM, and closed any remaining void pixels applying the MW method with a 3 × 3 pixel window. More advanced approaches are possible, which alter the surface of the original DEM (Dowding *et al.* 2004); however these were not implemented here. MW and FF are complementary in that MW is used where there is no auxiliary DEM, and FF is used where there is.

For TIN, which is by definition a triangular network of mass points with 3D-coordinates connected by edges to form a triangular tessellation, the weed tolerance (the minimal tolerance between two data points at a line) was set to 0.0001 of the maximum extent of the input data set, whereas the proximal tolerance (minimal distance between single data points) was set to the machine precision of the host computer.

The ANU approach (Hutchinson 1989, Hutchinson and Dowling 1991) is implemented in ArcInfo as TOPOGRID, and creates a hydrologically correct DEM using a multi-resolution iterative finite difference interpolation (extended spline) method, which ensures that ridges are maintained, streams are enforced and spurious sinks are removed. The ANU approach contains three parameters which are used for the smoothing of the input data and the removing of sinks (ESRI 2000). The TOL1 tolerance was initially set to 5 m (half the height difference between contours); however, if the maximum elevation difference observed in the data preparation dataset was below the contour interval, it was set to half that value. Values for the horizontal and vertical standard errors were set to one and zero respectively.

The authors limited the number of implementations to the above described algorithms, though even more advanced algorithms (Soile 1991, Hofer *et al.* 2006) look advantageous. If needed, more advanced algorithm e.g. conditioned simulations (Holmes *et al.* 2000) could be implemented in the processing chain.

3.3 Evaluation

For each void we applied the seven VF algorithms three times, once with no auxiliary data, and once each with the SRTM30 and GTOPO30 information, resulting in 21 DEMs, plus the reference DEM. A visual example of the results from each VF algorithm for a set of voids is shown in Figure 7. Figure 7a shows the void to be filled, whereas the other examples (b to i) present the different VF results. The effect of coarse resolution auxiliary data is clearly visible in Figure 7i with the Fill and Feather approach. In Figure 7h the extrapolation by moving window shows some limitation as extrapolation from the borders of the void occurs. The geostatistical algorithms in Figures 7d, e and f show only slightly different visual appearances, e.g. the representation of the peak on the left side of the large voids. Finally, the TIN and ANUDEM approaches show slightly different elevation surfaces, with TIN creating a ridge in the major void (Figure 7c), which is not visible in the hydrologically correct ANUDEM surface (Figure 7b).

We compared the elevation of the reference DEM (z_{Ref}) to the 21 DEM (z_{DEM}) by computing the Root Mean Square Error (RMSE), Pearson’s Correlation Coefficient (ρ), the average difference (μ), the sum difference (γ) and the standard deviation of the difference between both surfaces (σ). Additionally, we computed the area for each void.

We choose an evaluation based on the total area of the void similar to Grohman *et al.* (2006) in contrast to a selected number of GCP (Dowding *et al.* 2004).

The RSME was computed between the reference elevation and the 21 elevation surfaces. Each void filled DEM patch was ranked from 1 (lowest RMSE) to 7 - or 21 for a comparison across all variations - (highest RMSE). The distribution of the ranking relative to terrain and void size was assessed by summarising the ranking results by: (i) terrain unit, (ii) size class, (iii) terrain unit and size class and (iv) auxiliary datasets.

Fisher and Tate (2006) argue that the RMSE is not necessarily a good estimator of the error, recommending the mean error (ME) and the error standard deviation (S), where *n* is the number of pixels in the void:

$$ME = \frac{\gamma}{n}$$

$$S = \sqrt{\frac{\sum\left[(z_{Dem} - z_{\mathrm{Re}\,f}) - ME\right]^2}{n-1}}$$

We performed the comparative analysis based on RMSE, ME and S and observed consistent best VF results for different TU/Void size classes for RSME and S. ME showed diverse rankings of different algorithms. For the remaining course of this paper we provide results for RSME only, and discuss the S and ME results where appropriate. We are aware that a global statistic was used to compare the filled voids against the truth surface, rather than evaluation methods which take the spatial pattern of errors into account or which identify the different factors which led to that error.

4. Results

4.1. *Evaluation of the void filling algorithms with respect to terrain unit*

Table 3 shows the statistical summary of the ranking results when the void is classified by its terrain unit, irrespective of the size of the void. The Table 3 shows the mean and standard deviation (in parentheses) of the ranking of each VF method for each terrain unit, with and without an auxiliary DEM. The geostatistical method KR and the mechanical method SP (e.g. no assessment of the uncertainty of the model is possible) are consistently the "best" methods, with KR performing better in flatter areas (Plains, Plateaus and High Plateaus) and SP performing better in mountainous terrains (Hills, Mountains and High Mountains). Differences between VF methods in RMSE can triple (e.g. see first row differences between KR (6.04 and SP 17.40), which agrees with the Fisher and Tate (2006) statement that no single interpolation method exists that is the most accurate for the interpolation of terrain data.

Still, the "best" method in Table 3 sometimes contains groups of 2 different VF methods, almost similar in RSME results. An example is the VF for PLAINS without any auxiliary DEM, where KR (6.04) and IDW (6.44) show similar results (similar results = ± 1 RMSE difference). On the contrary SP, MW and ANU are the most variable in terms of performance. On the other hand, for certain TU, e.g. in HIGH MOUNTAINS, the algorithm SP (4.06) shows the "best" performance, with results of all other algorithms being quite different.

Related to that last observation, the standard deviation, which is larger than for all other VF methods in that TU, suggests that there were several voids where SP performed poorly. Therefore the SD is a good indicator of the general applicability of the VF algorithm for a given TU. In this case, it would be advisable to check further to identify cases, which are not well handled (e.g. it could be an effect of the void size) and to rerun the analysis.

Generally, the use of auxiliary information of the GTOPO30 dataset increased the RMSE for all VF methods except for small improvements in TR. This might be attributed to the different types of errors not accounted for in our methodology (see also section 1.2).

The use of SRTM30 as an auxiliary dataset decreased the RMSE/S for most case, and decreased the standard deviation indicating less variation in the level of improvement. This is not surprising since SRTM30 is an up-scaled and void-filled derivative of the SRTM data. One could argue that the use of SRTM30 should be preferred, however in practice this means that we are down-scaling data (SRTM30 to SRTM) from a previous up-scaling (SRTM to SRTM30)! This circularity may be acceptable in certain cases if we know how the SRTM30 data was generated in the area of the particular void we are filling. This problem is discussed further in section 5.2.1.

[Insert Table 3]

4.2. ***Evaluation of void filling methods with respect to void size***

Table 4 shows the statistical summary of the ranking results when the void is classified by size. Again, the table shows the mean and standard deviation (in parentheses) of the ranking of each VF method for each size class, with and without an auxiliary DEM. In this classification of voids, KR is consistently the best method for small and medium sized voids, regardless of the use of auxiliary data. If auxiliary data are used, KR performed best up to void size class F compared with up to void size class D without auxiliary information. The reason behind this is probably that the KR delivers an average elevation surface, which closer resembles the reference DEM, in contrast to the TIN dataset. In TIN the relationship between triangles and their adjacent neighbours are handled more stringently, more closely resembling the input dataset.

For large and very large voids, the inclusion of an auxiliary DEM has an obvious effect on the performance of the algorithms. TIN is better where there is no auxiliary information, IDW is better where GTOPO30 is used and TIN or ANU are best when SRTM30 is used. One might speculate on the differences between the auxiliary datasets. One possible explanation is that TIN/ANU requires 'good quality' auxiliary information, whereas IDW as a geostatistical algorithm generates an "average surface" as mentioned earlier.

[Insert Table 4]

4.3. Evaluation of void filling methods with respect to terrain unit and void size

Table 5 shows the best method for the final classification based on both terrain unit and void size, resulting in 48 possible void typologies, although as can be seen from Table 5a, six of these typologies contain no voids (High Plateaus in particular is a rare terrain unit) and the number of voids per typology varies from 80 to 3. Tables 5a to 5c show the best performing VF algorithm for each typology, again using no auxiliary DEM (Table 5a), GTOPO30 (Table 5b) and SRTM30 (Table 5c). The table cells are shaded to help interpretation.

The first observation is that KR outperforms any other VF algorithm for very small voids (Class A), except in High Mountains, where SP is better. Secondly, for very large voids in mountainous terrain (arguably the most difficult voids to interpolate), ANU and TIN are the best, with ANU being superior when SRTM30 is used. Other noticeable trends include IDW in planar areas for large voids with no DEM or GTOPO30, and SP for medium to large voids (Classes C to F) for all terrain units except Plains, and especially for Mountains and High Mountains.

A test of the SD of the RSME for the different methods showed a similar distribution across all VF methods, void sizes and terrain units, which allows us to be quite confident in the results presented here. One exception is however for the largest void class (H) in the terrain unit PLAINS and PLATEAUS for the VF method SP. The reason for that exception might be attributed to the relatively low number of investigated voids in that class.

[Insert Table 5]

Looking across tables 5a to 5c, the use of coarse resolution auxiliary DEM data has little or no impact on the results for void size classes A through D, but the possible inclusion of such auxiliary information becomes important for the larger void classes (E through H). If a VF algorithm is to be recommended for these void sizes for global application, then we must differentiate between the three choices for auxiliary information.

Table 5d shows the best performing VF algorithm and the auxiliary information that was used for all terrain units for size classes E through H. Looking only at the auxiliary DEM results, we can see that SRTM30 is the preferred auxiliary DEM for very large voids (size classes G and H), whilst there is no one recommended auxiliary DEM for classes E and F. Looking at the VF method and auxiliary information together, KR always uses SRTM30, and ANU always uses SRTM30, except for the PLAINS, where a variety of methods is recommended based on the void size class. A mixture of VF algorithm is recommended for medium size voids (E-F) based on the TU (IDW for Plains, TIN for HILLS, and SP/ANU for the remaining TU).

It is interesting to see that certain algorithms deliver the best results without auxiliary information (e.g. recommending SP without any auxiliary information for size class F in high plateaus). Further investigation is required to determine why the errors without auxiliary information are less than with VF algorithms that use auxiliary information. One reason might be that we a have not sufficiently compensated for the errors in the dataset (c.f section 1.2) during the preparation of input data for the VF and this may bias the results. Another observation is that most of the recommended VF algorithms create a smooth surface which stays within the elevation range of the input data. This means that mountain ridges for example can not be represented properly, even if the RMSE/ME proves that the approximation is best for the VF patch, and that the local noise structure of the surrounding area is smoothed out. Finally, GTOPO30 is derived from a range of topographic sources, and the variation in quality of these sources across Africa is likely to have an impact on these results.

4.4. *Evaluation of void filling methods with respect to auxiliary information*

To determine if the inclusion of low quality auxiliary information has any improvement on the VF algorithms, for each void we computed the percentage difference between the RSME with no auxiliary information and (i) RMSE with SRTM30 and (ii) RMSE with GTOPO30. The results are summarised by void size class and terrain (Table 6) for all void sizes E through H.

Percentages lower than 100 indicate that the inclusion of auxiliary information resulted in an improvement and vice versa. A percentage equal to 100 means that the first restriction of the area threshold (c.f. Section 2.5) has been met, however due to the second restriction (e.g. the shape of the void) the auxiliary data has not been used.

As expected, overall, SRTM30 improves the VF results more than GTOP30, but surprisingly both auxiliary datasets also degrade the VF results in several cases (e.g. in mid-sized voids and in some terrain units - Table 6). This suggests that the area threshold should depend on the TU. For example, for VF algorithm KR in MOUNTAINS using GTOPO30, an increase in accuracy can only be observed if the void area is larger than void size class F. Below that void size class, GTOPO30 did not improve the VF results and even decreases accuracy. For GTOPO30, the area threshold should be only the largest class (H) for PLAINS, LOW PLATEAUS, HILLS and HIGH MOUNTAIN. For HIGH PLATEAUS no recommendation can be given (or even not to use coarse scale auxiliary information), and for MOUNTAINS the area threshold should be class G.

SRTM30 not surprisingly outperforms GTOPO30. Generally, the largest improvements for SRTM30 occur in large and very large void sizes (G and H). Similarly to GTOPO30, the area thresholds and when to use auxiliary information vary. For PLAIN, LOW PLATEAU and MOUNTAINS the void size class G is recommended; for HIGH PLATEAUS again no recommendation can be given and for HILLS and HIGH MOUNTAIN the area threshold should be set to H.

These results indicate that such coarse resolution auxiliary data is generally only applicable to extremely large voids, and highlights the need to use higher resolution auxiliary datasets in the void filling the SRTM data, rather than the SRTM30 and GTOPO30 datasets used here.

[Insert Table 6]

4.5 Application of the 'best' VF methods to the global SRTM data

One of the objectives of this paper has been to provide a worldwide database of voids, in which each void has an assigned "best" method based on terrain unit and void size. This has been performed based on the results in Table 5, and the database will be provided to the international user community at http://srtm.jrc.it/ and http://srtm.csi.cgiar.org/. The International Centre for Tropical Agriculture (CIAT), through the Consortium for Spatial Information (CSI), has been providing ready to use seamless (i.e. void filled) SRTM elevation data since 2003. These derived data have been gradually improved over three versions through the use of better interpolation algorithms (currently ANUDEM) and auxiliary DEMs.

The database of "best" VF methods could be used to create a fourth version of the seamless SRTM elevation data by identifying the voids where there is no high resolution auxiliary DEM information available (which is currently the vast majority of voids), and by then applying the recommended VF algorithm to the remaining voids. Where high resolution DEMs are available we recommend the ANUDEM procedure.

5. Conclusions

5.1. *General conclusions*

The authors assume that each void occurs due to a technical reason, which can be partly attributed to terrain, land use and other reasons. In the course of this analysis, void areas in the SRTM data set have been quantified in terms of their terrain and size, providing a statistically sound and extensive evaluation of different VF algorithms over a wide range of terrain units and void sizes (objective i).

Different VF algorithms have been implemented in a GIS, and used to analyse performance using RMSE/S on 1,304 relocated voids. Based on these results a decision table has been created, which provides an answer to an important question: which VF method can be recommended for a void of a given size in a given terrain unit? Contrary to some previous findings, the best methods can be generalised as: Kriging or Inverse Distance Weighting interpolation for small and medium size voids in relatively flat low-lying areas; Spline interpolation for small and medium sized voids in high altitude and dissected terrain; Triangular Irregular Network or Inverse Distance Weighting interpolation for large voids in very flat areas, and an advanced spline method (ANUDEM) for large voids in other terrains (objectives ii and iv).

We have shown that coarse resolution auxiliary information was only helpful if the void areas exceeded a certain size threshold (objective iii). Differences in decrease of RMSE could be observed between use of the SRTM30 and the GTOPO30 DEMs.

Finally, we have created a database that can be used to select a VF algorithm and auxiliary DEM to fill each of the 3,339,913 voids in the SRTM data (objective v).

5.2. *Further work*

5.2.1 Issues with the SRTM30 data. In this paper we tested only coarser scale resolution data as auxiliary information for the VF process. The VF using the SRTM30 obviously creates a better result than using GTOPO30 auxiliary information (Table 3). Still, SRTM30 is a seamless DEM based on the SRTM data product and is therefore also influenced by the voids. Most voids in the underlying SRTM data were interpolated in a 10 × 10 averaging process that re-sampled the data from 3 seconds to 30 seconds. Voids that were too large to be interpolated in this manner were filled using GTOPO30.

Since the SRTM data does not have global coverage, GTOPO30 data from areas above 60ºN and below 56ºS were fused with the SRTM data to create the final SRTM30 data. No attempt was made to adjust the vertical datum of either dataset in this fusion. There are three observations to be made here. Firstly, the SRTM30 product will have variable quality in areas where there were reasonably large voids within the 10 × 10 re-sampling window. Secondly, there is no advantage in using SRTM30 instead of GTOPO30 as an auxiliary DEM for interpolating very large voids since the auxiliary information in these areas will be almost identical. Thirdly, if the recommended VF algorithms and all available auxiliary datasets are used to create a seamless 3 second SRTM dataset (as would be the case in a fourth version of the CSI SRTM data), this in turn can be used to create a higher quality SRTM30 dataset and other global coarse resolution derivatives.

5.2.2 Size thresholds for auxiliary data. A second question is the size of thresholds for higher resolution auxiliary datasets, which might influence results quite significantly. A conservative threshold for using auxiliary elevation information (void size class D) has been applied which was obviously not large enough (Table 6) under certain conditions. Further research is required to provide better information on the required resolution and quality of auxiliary DEMs for filling voids of different sizes.

5.2.3 High resolution auxiliary data. We assume that high resolution DEM data (e.g. based on ASTER or SPOT satellite derived data, or digitised from fine-scale topographic maps) should deliver superior results for void filling as the density and distribution of the auxiliary data is superior. The degree of improvement offered by these data has to be offset against the time and the cost of acquiring and processing such information. Higher resolution may not necessarily mean higher quality; relative ASTER DEM products show height differences of up to 600 meters between three different scenes for the same area and other ASTER DEM errors are specified in Lönnqvist and Törmä (2004). Inherent to the use of auxiliary information is the question of how different errors can automatically be compensated for, as outlined in section 1.2.

5.2.4 Better understanding of void filling algorithms. This analysis has treated the VF algorithms as black boxes in that we have only looked at the results of the interpolation accuracy rather than attempted to investigate the reasons why one method performs better than another. Interrogation and analysis of the inner workings of these algorithms under different conditions would be a valuable aid to researchers who need to select an appropriate method for a given problem.

Acknowledgement and disclaimer

We are grateful to the two anonymous reviewers for their constructive comments on this paper. International boundaries are illustrative only. Names of commercial products or manufacturers are for information purposes only and do not imply endorsement or commendation. This article includes a word that is or is asserted to be a proprietary term or trade mark. Its inclusion does not imply it has acquired for legal purposes a non-proprietary or general significance, nor is any other judgement implied concerning its legal status.

References

ALMANSA, A., CAO, F., GOUSSEAU, Y. and ROUGE, B., 2002, Interpolation of digital elevation models using AMLE and related methods, *IEEE Transactions on Geoscience and Remote Sensing*, **40(2)**, pp. 314-325

CHAPLOT, V., DARBOUX, F., BOURENNANE, H., LEGUEDOIS, S., SILVERA, N. and PHACHOMPHON, K., 2006, Accuracy of interpolation techniques for the derivation of digital elevation models in relation to landform types and data density, *Geomorphology,* **77**, pp. 126-41.

COLTELLI, M., FORNARO, G., FRANCESCHETTI, G., LANARI, R., MIGLIACCIO, M., MOREIRA, J. R., PAPATHANASSIOU, K. P., PUGLISI, G., RICCIO, D. and SCHWABISCH, M., 1996, SIR-C/X-SAR multifrequency multipass interferometry: A new tool for geological interpretation, *Journal of Geophysical Research,* **101**, pp. 23127-48.

DOWDING, S., KUUSKIVI, T. and LI, X., 2004, Void fill of SRTM elevation data – Principles, Processes and Performance, Available online at: www.intermap.com/images/papers/void_fill_paper_fall_asprs_2004.pdf (accessed 01/07/2006).

EINEDER, M., 2005, Interferometric DEM Reconstruction of Alpine Areas – Experiences with SRTM Data and Improved Strategies for Future Missions, Available online at: www.ipi.uni-hannover.de/html/aktivitaeten/EARSeL-Workshop2005_Paper/Eineder.pdf (accessed 01/08/2006).

ESRI, 2000, *ArcInfo User's Guide*, (Redlands, California: Environmental Systems Research Institute).

FALORNI, G., TELES, V., VIVONI, E. R., BRAS, R. L. and AMARATUNGA, K., 2005, Analysis and characterization of the vertical accuracy of digital elevation models from the shuttle radar topography mission, *Journal of Geophysical Research - Earth Surface,* **110**, F02005, pp.1-20.

FARR, T. G. and KOBRICK, M., 2000, Shuttle Radar Topography Mission produces a wealth of data, *American Geophysical Union,* **81**, pp. 583-85.

FISHER, P. F. and TATE, N. J., 2006, Causes and consequences of error in digital elevation models, *Progress in Physical Geography,* **30**, pp. 467-89.

FRANKE, R., 1982, Smooth Interpolation of Scattered Data by Local Thin Plate Splines, *Comp. & Maths. with Appls,* **8**, pp. 237-81.

GAMACHE, M., 2004, Free and Low Cost Datasets for International Mountain Cartography, Available online at: www.icc.es/workshop/abstracts/ica_paper_web3.pdf (accessed 01/08/2006).

GROHMANN, G., KROENUNG, G. and STREBECK, J., 2006, Filling SRTM Voids: The Delta Surface Fill Method, *Photogrammetric Engineering & Remote Sensing,* **72**, pp. 213-16.

HASTINGS, D. A. and DUNBAR, P. K., 1998, Development and assessment of the Global Land One-km Base Elevation Digital Elevation Model (GLOBE), *International Society of Photogrammetry and Remote Sensing Archives,* **32**, pp. 218-21.

HENGL, T. and EVANS, I. S., 2007, Geomorphometry: A brief guide. In *Geomorphometry: Concepts, software, applications*, T. Hengl and H. I. Reuter (Eds.) (Ispra, Italy: European Commission, 2007), pp. 3-18.

HOFER, M., SAPIRO, G. and WALLNER, J., 2006, Fair polyline networks for constrained smoothing of Digital Terrain Elevation Data, *IEEE Transaction on Geoscience and Remote Sensing*, **10**, pp. 1-8.

HOLMES, K.W., CHADWICK, O.A. and KYRIAKIDIS, P.C. 2000, Error in a USGS 30 m DEM and its impact on terrain modeling. *Journal of Hydrology,* **233**, pp. 154–73.

HUTCHINSON, M. F., 1989, A new procedure for gridding elevation and stream line data with automatic removal of spurious pits, *Journal of Hydrology,* **106**, pp. 211-32.

HUTCHINSON, M. F. and DOWLING, T. I., 1991, A continental hydrological assessment of a new grid-based digital elevation model of Australia, *Hydrological Processes,* **5**, pp. 45-58.

KAAB, A., 2005, Combination of SRTM3 and repeat ASTER data for deriving alpine glacier flow velocities in the Bhutan Himalaya, *Remote Sensing of Environment,* **94**, pp. 463-74.

KATZIL, Y. and DOYTSHER, Y., 2000, Height estimation methods for filling gaps in gridded DTM, *Journal of Photogrammtric Enginerring,* **126**, pp. 145-62.

KERVYN, F., 2001, Modelling topography with SAR interferometry: illustrations of a favourable and less favourable environment, *Computers and Geosciences,* **27**, pp. 1039-50.

KUUSKIVI, T., LOCK, J., LI, X., DOWDING, S. and MERCER, B., 2005, Void Fill of SRTM Elevation Data: Performance Evaluations, Available online at: www.intermap.com/images/papers/void_fill.pdf (accessed 01/07/2006).

LÖNNQVIST, M. and TÖRMÄ, M., 2004, Different Implications of Spatial Boundary - Jebel Bishri between the Desert and the Sown on Syria, Available online at: www.isprs.org/istanbul2004/comm3/papers/397.pdf (accessed 01/07/2006).

MACMILLAN, R. A., PETTAPIECE, W. W., NOLAN, S. C. and GODDARD, T. W., 2000, A generic procedure for automatically segmenting landforms into landform elements using DEMs, heuristic rules and fuzzy logic, *Fuzzy Sets and Systems,* **113**, pp. 81-109.

MCBRATNEY, A. B. and WEBSTER, R., 1986, Choosing Functions for Semi-variograms of Soil Properties and Fitting Them to Sampling Estimates, *Journal of Soil Science,* **37**, pp**.** 617-39.

MEYBECK, M., GREEN, P. and VOROSMARTY, C., 2001, A New Typology for Mountains and Other Relief Classes: An Application to Global Continental Water Resources and Population Distribution, *Mountain Research Development,* **21**, pp. 34-45.

MITAS, L. and MITASOVA, H., 1988, General Variational Approach to the Interpolation Problem, *Comput. Math. Applic,* **16**, pp. 983-92.

MITASOVA, H. and HOFIERKA, J., 1993, Interpolation by regularized spline with tension, *Mathematical Geology,* **25**, pp. 657-69.

RABUS, B., EINEDER, M., ROTH, A. and BAMLER, R., 2003, The shuttle radar topography mission--a new class of digital elevation models acquired by spaceborne radar, *ISPRS Journal of Photogrammetry and Remote Sensing,* **57**, pp. 241-62.

RODRIGUEZ, E., MORRIS, C. S., BELZ, J. E., CHAPIN, E. C., MARTIN, J. M., DAFFER, W. and HENSLEY, S., 2005, An assessment of the SRTM topographic products, Technical Report JPL D-31639, Jet Propulsion Laboratory, Pasadena, California, pp. 143.

RODRIGUEZ, E., MORRIS, C. S., and BELZ, J. E., 2006, A global assessment of the SRTM Performance, Photogrammetric Engineering & Remote Sensing, 72(3), pp. 249-260.

SHARF, A., ALEXA, M. and COHEN-ORR, D., 2004, Context based surface completion, *ACM Trans. Graph.,* **23**, pp. 878-87.

SOILE, P., 1991, Spatial Distributions from Contour Lines: An Efficient Methodology Based on Distance Transformations, *Journal of Visual Communication and Image Representation,* **2**, pp. 138-50.

SLATER, J.A., GARVEY, G., JOHNSTON, C., HAASE, J., HEADY, B., KROENUNG, G. AND LITTLE, J., 2006, The SRTM Data Finishing Process and Products. *Photogrammetric Engineering and Remote Sensing,* **772(3)**, pp. 237-248.

THAPA, K. and BOSSLER, J., 1992, Accuracy of spatial data used in geographical information systems. *Photogrammetric Engineering and Remote Sensing,* **58**, pp. 835–41.

TOUTIN, T., 2002, Impact of terrain slope and aspect on radargrammetric DEM accuracy, *Journal of Photogrammetry and Remote Sensing*, **7**, pp. 228-40.

USGS, 1996, GTOPO30 (Global 30 Arc-Second Elevation Data Set), Available online at: http://edc.usgs.gov/products/elevation/gtopo30.html (accessed 01/08/2006).

USGS, 2006a, Shuttle Radar Topography Mission (SRTM) "Finished" 3-arc second SRTM Format Documentation, Available online at: http://edc.usgs.gov/products/elevation/srtmbil.html (accessed 01/08/2006).

USGS, 2006b, Shuttle Radar Topography Mission DTED® Level 1 (3-arc second) documentation, Available online at: http://edc.usgs.gov/products/elevation/srtmdted.html (accessed 01/08/2006).

USGS, 2006c, Shuttle Radar Topography Mission Water Body Dataset, Available online at: http://edc.usgs.gov/products/elevation/swbd.html (accessed 01/08/2006).

USGS, 2006d, SRTM30 Documentation, Available online at: ftp://e0srp01u.ecs.nasa.gov/srtm/version2/SRTM30 (accessed 01/08/2006).

VEDERA, J., CASELLES, V., BERTALMIO, M. and SAPIRO, G., 2003, Inpainting surface holes. In *Int. Conference on Image processing (ICIP 2003)*, pp. 903-06.

VERDIN, K. L. and GREENLEE, S. K., 1996, Development of continental scale digital elevation models and extraction of hydrographic features., Available online at: http://ncgia.ucsb.edu/conf/SANTA_FE_CD-ROM/sf_papers/verdin_kristine/santafe2.html (accessed 01/08/2006).

WATSON, D. F. and PHILIP, G. M., 1985, A Refinement of Inverse Distance Weighted Interpolation, *Geo-Processing*, **2**, pp. 315-27.

WERNER, M., 2001, Shuttle Radar Topography Mission (SRTM), Mission overview *Journal of Telecommunication (Frequenz),* **55**, pp. 75-79.

YANG, X. and HODLER, T. 2000, Visual and statistical comparisons of surface modeling techniques for point-based environmental data. *Cartography and Geographic Information Science* **27**, pp. 165–75.

Table 1. Number of global voids by terrain unit and void size (A-H).

	A	B	C	D	E	F	G	H	Sum
PLAINS	458,851	27,968	7,414	3,746	1,810	1,453	552	437	502,231
PLATEAUS	765,745	54,739	13,700	5,425	1,831	965	223	67	842,695
H. PLATEAUS	24,056	1,082	278	171	107	128	91	85	25,998
HILLS	195,055	13,097	3,286	1,157	339	157	21	5	213,117
MOUNTAINS	789,587	58,258	15,673	6,319	2,125	1,108	228	51	873,349
H. MOUNTAINS	680,952	53,497	15,825	7,235	2,869	1,888	523	154	762,943
Sum	2,914,246	208,641	56,176	24,053	9,081	5,699	1,638	799	3,220,333*

* The total number of voids in this table does not sum to 3,399,913 due to some voids not being assigned terrain units. The vast majority of these unassigned voids are in coastal areas and should be classed as PLAINS.

Table 2. Number of artificial voids by terrain unit and void size (A-H)

	A	B	C	D	E	F	G	H	Sum
PLAINS	45	45	60	60	45	15	15	15	300
PLATEAUS	65	60	75	80	60	20	28	12	400
H. PLATEAUS	30	40	40	40	35	10	5	0	200
HILLS	15	20	25	20	20	0	0	0	100
MOUNTAINS	30	40	39	40	30	10	14	6	209
H. MOUNTAINS	15	15	20	30	5	5	5	0	95
Sum	200	220	259	270	195	60	67	33	1,304

Table 3. Mean and standard deviation (in brackets) of the RMSE ranking for each method by terrain unit. Best results are in bold.

No auxiliary DEM

	KR*	SP	TR	IDW	MW	TIN	ANU
	6.04	17.40	9.79	6.44	10.6	8.52	10.00
PLAINS	**(3.82)**	(4.15)	(5.60)	(3.76)	(5.06)	(4.66)	(5.18)
	5.71	9.79	16.40	10.50	10.70	6.74	7.02
PLATEAUS	**(4.12)**	(6.75)	(3.76)	(3.83)	(4.21)	(3.91)	(4.37)
	5.18	6.23	17.50	11.50	11.10	6.88	7.01
H. PLATEAUS	**(3.56)**	(6.24)	(2.06)	(3.07)	(3.35)	(3.53)	(4.04)
	5.79	**5.36**	17.50	11.50	10.70	7.01	8.36
HILLS	(4.39)	**(5.62)**	(2.18)	(3.35)	(3.95)	(3.41)	(4.17)
	5.95	**5.16**	17.10	12.20	11.30	7.14	7.78
MOUNTAINS	(3.82)	**(5.77)**	(3.35)	(2.99)	(3.29)	(3.83)	(3.81)
	5.97	**4.06**	17.50	12.90	12.60	6.46	8.24
H. MOUNTAINS	(3.50)	**(4.93)**	(2.28)	(2.46)	(2.79)	(3.31)	(3.95)

GTOPO30

	KR	SP	TR	IDW	FF	TIN	ANU
	7.25	17.50	9.74	6.44	15.70	10.40	11.8
PLAINS	**(4.72)**	(4.02)	(5.51)	(3.76)	(6.48)	(5.30)	(5.39)
	6.00	10.20	16.30	10.50	18.60	7.75	7.72
PLATEAUS	**(4.24)**	(6.98)	(3.69)	(3.82)	(4.37)	(4.54)	(4.74)
	5.83	6.86	17.20	11.50	19.60	8.20	7.94
H. PLATEAUS	**(4.27)**	(6.83)	(2.23)	(3.06)	(2.46)	(4.21)	(4.46)
	5.83	**5.71**	17.40	11.50	19.30	7.25	8.44
HILLS	(4.31)	**(5.90)**	(2.17)	(3.36)	(3.40)	(3.54)	(4.28)
	6.39	6.90	17.00	12.20	17.90	8.35	8.54
MOUNTAINS	**(4.33)**	(7.26)	(3.15)	(2.98)	(4.79)	(4.59)	(4.03)
	6.14	**4.47**	17.40	12.90	18.60	6.91	8.53
H. MOUNTAINS	(3.83)	**(5.77)**	(2.33)	(2.46)	(3.83)	(3.86)	(4.05)

SRTM30

	KR	SP	TR	IDW	FF	TIN	ANU
	5.67	16.70	9.65	6.44	10.00	7.97	9.97
PLAINS	**(3.79)**	(4.30)	(5.49)	(3.76)	(6.38)	(4.98)	(5.31)
	5.28	9.34	16.20	10.50	15.50	6.65	6.69
PLATEAUS	**(3.93)**	(6.39)	(3.72)	(3.82)	(5.58)	(3.99)	(4.49)
	5.22	5.94	17.30	11.50	17.20	7.43	7.36
H. PLATEAUS	**(3.48)**	(6.03)	(2.20)	(3.06)	(3.78)	(3.81)	(4.18)
	5.68	**5.39**	17.40	11.50	16.30	6.88	8.30
HILLS	(4.23)	**(5.51)**	(2.14)	(3.36)	(4.49)	(3.45)	(4.30)
	5.49	**5.02**	17.00	12.20	15.50	6.97	7.50
MOUNTAINS	(3.86)	**(5.49)**	(3.22)	(2.98)	(4.74)	(4.05)	(4.03)
	5.63	**3.86**	17.50	12.90	16.70	6.38	8.00
H. MOUNTAINS	(3.30)	**(4.49)**	(2.18)	(2.46)	(3.99)	(3.29)	(4.07)

* Methods are Kriging (KR), Spline (SP), Trend (TR), Inverse Distance Weighting (IDW), Moving Window Average (MW), Fill and Feather (FF), Triangulated Irregular Network (TIN), and ANUDEM (ANU).

Table 4. Mean and standard deviation (in brackets) of the RSME ranking for each method by void size class. Best results are in bold.

	No auxiliary DEM						
	KR*	SP	TR	IDW	MW	TIN	ANU
A	**6.20**	16.60	9.26	6.94	10.60	9.01	10.00
	(3.84)	(4.74)	(5.97)	(3.89)	(5.45)	(4.89)	(5.45)
B	**5.56**	14.40	13.00	7.66	10.70	7.94	9.16
	(3.99)	(6.74)	(5.23)	(4.52)	(4.71)	(4.40)	(4.82)
C	**5.74**	9.77	16.80	10.70	10.70	6.27	6.70
	(4.05)	(6.74)	(3.30)	(3.53)	(3.89)	(3.48)	(4.18)
D	5.74	**4.49**	17.70	12.00	11.00	6.89	8.15
	(4.28)	**(4.95)**	(1.35)	(2.99)	(3.70)	(3.26)	(4.10)
E	**5.52**	5.33	17.30	12.00	11.40	7.15	7.80
	(3.88)	(5.73)	(2.77)	(3.16)	(3.39)	(3.81)	(4.05)
F	6.62	**5.86**	16.70	11.60	9.95	6.67	6.41
	(3.50)	**(5.97)**	(4.29)	(2.95)	(2.84)	(3.80)	(3.23)
G	5.68	**4.22**	17.60	12.80	12.70	6.74	9.07
	(3.36)	**(5.64)**	(1.72)	(2.48)	(2.98)	(3.40)	(3.85)
H	7.20	6.36	17.40	13.00	12.60	**6.00**	6.16
	(3.64)	(6.53)	(3.24)	(2.37)	(2.32)	**(3.01)**	(3.14)
	GTOPO30						
	KR	SP	TR	IDW	FF	TIN	ANU
A	**6.53**	16.80	9.16	6.94	14.80	9.65	10.60
	(4.15)	(4.69)	(5.93)	(3.89)	(7.07)	(5.35)	(5.56)
B	**6.89**	14.40	13.00	7.66	16.30	10.10	11.00
	(5.03)	(6.66)	(5.11)	(4.51)	(5.94)	(5.12)	(5.43)
C	**6.14**	10.30	16.60	10.70	19.60	7.55	7.62
	(4.25)	(7.05)	(3.22)	(3.53)	(2.78)	(4.44)	(4.68)
D	5.75	**4.81**	17.60	11.90	19.50	7.13	8.22
	(4.20)	**(5.28)**	(1.37)	(2.99)	(2.54)	(3.40)	(4.21)
E	**5.83**	5.64	17.20	12.00	18.00	7.77	8.23
	(4.19)	(6.08)	(2.82)	(3.16)	(4.85)	(4.14)	(4.19)
F	**8.31**	12.00	16.20	11.60	19.80	10.70	8.91
	(4.81)	(8.39)	(3.62)	(2.92)	(1.63)	(5.32)	(4.31)
G	5.57	**4.11**	17.50	12.80	17.90	7.00	9.20
	(3.26)	**(5.41)**	(1.79)	(2.48)	(4.26)	(3.65)	(3.87)
H	7.73	7.66	16.90	13.00	20.00	**7.43**	7.10
	(4.44)	(8.02)	(3.30)	(2.37)	(1.66)	**(4.65)**	(3.99)
	SRTM30						
	KR	SP	TR	IDW	FF	TIN	ANU
A	**6.26**	16.5	9.21	6.94	10.50	8.85	10.10
	(3.84)	(4.74)	(5.94)	(3.89)	(6.51)	(5.06)	(5.47)
B	**4.96**	13.40	12.80	7.66	11.20	7.35	8.90
	(3.81)	(6.37)	(5.21)	(4.51)	(6.83)	(4.65)	(5.00)
C	**5.21**	9.20	16.60	10.70	16.00	6.15	6.32
	(3.84)	(6.29)	(3.24)	(3.53)	(5.00)	(3.59)	(4.29)

D	5.64	**4.51**	17.70	11.90	16.80	6.79	8.09
	(4.12)	**(4.82)**	(1.30)	(3.00)	(3.87)	(3.30)	(4.22)
E	5.53	**5.21**	17.20	12.00	16.60	7.43	7.96
	(3.85)	**(5.63)**	(2.81)	(3.16)	(4.36)	(3.93)	(4.09)
F	**5.65**	6.65	16.30	11.60	14.70	6.46	5.95
	(3.80)	(6.48)	(3.89)	(2.92)	(4.01)	(4.38)	(3.46)
G	5.17	**3.15**	17.50	12.80	16.20	6.38	8.64
	(3.31)	**(3.50)**	(1.75)	(2.48)	(5.12)	(3.49)	(4.30)
H	6.10	**5.73**	17.20	13.00	16.00	5.76	5.40
	(3.28)	**(5.66)**	(2.99)	(2.37)	(3.49)	(2.89)	(3.08)

* Methods are Kriging (KR), Spline (SP), Trend (TR), Inverse Distance Weighting (IDW), Moving Window Average (MW), Fill and Feather (FF), Triangulated Irregular Network (TIN), and ANUDEM (ANU).

Table 5. Best method results in terms of average rank by terrain unit and void size using (a) no auxiliary DEM, (b) GTOPO30 auxiliary data, (c) SRTM30 auxiliary data, and (d) across all data methods.

(a) No auxiliary Terrain unit	Void size A	B	C	D	E	F	G	H
PLAINS	KR* 6.11	IDW 6.11	KR 5.70	KR 6.95	IDW 4.43	IDW 4.66	KR 4.80	TIN 5.00
PLATEAUS	KR 5.92	KR 4.98	KR 4.48	SP 5.34	ANU 4.31	ANU 5.30	ANU 5.60	TIN 6.75
H. PLATEAUS	KR 3.33	SP 3.65	SP 4.75		TIN 5.05			
HILLS	KR 4.83	KR 4.07	KR 4.05	ANU 4.40	SP 1.57	SP 4.80	MW 5.20	
MOUNTAINS	KR 5.30	KR 4.97	SP 3.84	SP 1.55	SP 4.86	TIN 6.00	TIN 4.88	ANU 8.33
H. MOUNTAINS	SP 2.40	KR 4.40	SP 2.35	SP 2.40	SP 2.40	ANU 2.20	TIN 7.20	

(b) GTOPO30 Terrain unit	Void size A	B	C	D	E	F	G	H
PLAINS	KR 6.11	IDW 6.11	KR 5.70	IDW 7.51	IDW 4.42	IDW 4.66	IDW 5.53	IDW 8.00
PLATEAUS	KR 5.82	KR 4.98	KR 4.48	SP 5.29	ANU 5.53	KR 6.80	IDW 8.18	KR 9.72
H. PLATEAUS	KR 3.36	SP 3.65	SP 4.75		IDW 8.95			
HILLS	KR 4.83	KR 3.90	KR 4.05	ANU 4.40	SP 1.51	ANU 7.60	ANU 6.80	
MOUNTAINS	KR 5.30	KR 4.95	SP 3.84	SP 1.55	KR 7.06	KR 9.50	ANU 9.94	KR 7.00
H. MOUNTAINS	SP 2.40	KR 4.40	SP 2.35	SP 2.40	SP 2.40	IDW 10.60	ANU 4.60	

(c) SRTM30 Terrain unit	Void size A	B	C	D	E	F	G	H
PLAINS	KR 6.11	IDW 6.11	KR 5.70	KR 6.80	IDW 4.42	KR 4.00	KR 3.00	TIN 2.33
PLATEAUS	KR 5.77	KR 4.98	KR 4.48	SP 5.29	ANU 4.30	KR 4.95	ANU 3.53	ANU 1.83
H. PLATEAUS	KR 3.60	SP 3.65	SP 4.75		KR 5.90			
HILLS	KR 4.83	KR 4.02	KR 4.05	ANU 4.40	SP 1.57	KR 5.80	ANU 1.60	
MOUNTAINS	KR 5.30	KR 4.95	SP 3.84	SP 1.55	KR 4.86	KR 4.30	ANU 4.88	ANU 1.00
H. MOUNTAINS	SP 2.40	KR 4.4	SP 2.35	SP 2.40	SP 2.40	ANU 3.80	ANU 1.60	

(d) All cases**

Terrain unit	A	B	C	D	E	F	G	H
PLAINS					IDW + no aux	KR + sr30	KR + sr30	TIN + sr30
PLATEAUS					ANU+ sr30	KR + sr30	ANU+ sr30	ANU+ sr30
H. PLATEAUS					SP + gt30	SP + no aux	ANU+ sr30	
HILLS					TIN + noaux			
MOUNTAINS					SP + noaux	TIN + sr30	ANU+ sr30	ANU+ sr30
H. MOUNTAINS					SP + gt30	ANU+ noaux	ANU+ sr30	

* Methods are Moving Window Average (MW), Kriging (KR), Spline (SP), Inverse Distance Weighting (IDW), Triangulated Irregular Network (TIN), and ANUDEM (ANU).

** No auxiliary DEM (no aux), SRTM30 (sr30) and GTOPO30 (gt30).

Table 6. Average reduction in RMSE (in %) when auxiliary DEMs are used. Methods are Kriging (KR), Spline (SP), Triangulated Irregular Network (TIN), and ANUDEM (ANU).

Terrain	VF	GTOPO30				SRTM30			
Unit	Method	E	F	G	H	E	F	G	H
PLAINS	KR	143	118	161	192	109	100	91	72
	SP	141	114	103	35	99	87	59	16
	TIN	171	144	218	279	107	100	99	89
	ANU	183	157	210	273	114	103	99	96
PLATEAUS									
	KR	105	103	119	107	99	94	95	87
	SP	110	134	157	84	99	105	96	58
	TIN	111	120	130	121	101	105	94	82
	ANU	107	115	126	120	100	100	94	81
HIGH PLATEAUS									
	KR	121				104			
	SP	138				100			
	TIN	144				120			
	ANU	128				112			
HILLS									
	KR	100	100	110	100	100	100	102	97
	SP	100	100	162	78	100	100	118	71
	TIN	100	100	112	106	100	100	101	94
	ANU	100	100	105	104	100	100	103	91
MOUNTAINS									
	KR	100	127	81		100	93	72	
	SP	100	161	137		100	101	84	
	TIN	100	155	94		100	114	77	
	ANU	100	149	85		100	120	71	
HIGH MOUNTAINS									
	KR	112	116	121	86	93	95	100	61
	SP	239	161	207	62	134	107	140	37
	TIN	122	137	235	91	95	100	180	64
	ANU	114	118	205	90	95	97	162	63

Figure captions

Figure 1. The global distribution of voids in the SRTM data, represented by the proportion of void area in each 1 × 1 degree SRTM tile. Note the clustering of voids over mountainous and desert areas and the northern extent of the SRTM data (60ºN)

Figure 2. Voids (in black) overlaid on the SRTM30 elevation data for two extreme cases, Libya (upper) and Nepal (lower). The 1 × 1 degree SRTM tile boundaries have also been superimposed to express scale. The key shows elevation in metres above mean sea level.

Figure 3. Log log plot of the void size against the frequency distribution for the global void dataset (n= 3,339,913).

Figure 4. A 15 class terrain typology for Africa, based on the methodology proposed by Meybeck *et al.* (2000).

Figure 5. Percentage of voids per terrain unit and void size class for the global dataset.

Figure 6. Flow diagram of the VF algorithm assessment methodology.

Figure 7. Examples of the VF algorithms applied to a test area (a) in the SRTM DEM. The methods are (b) TOPOGRID, (c) TIN, (d) IDW, (e) Spline, (f) Kriging, (g) Trend, (h) Moving Average, and (i) Fill and Feather.

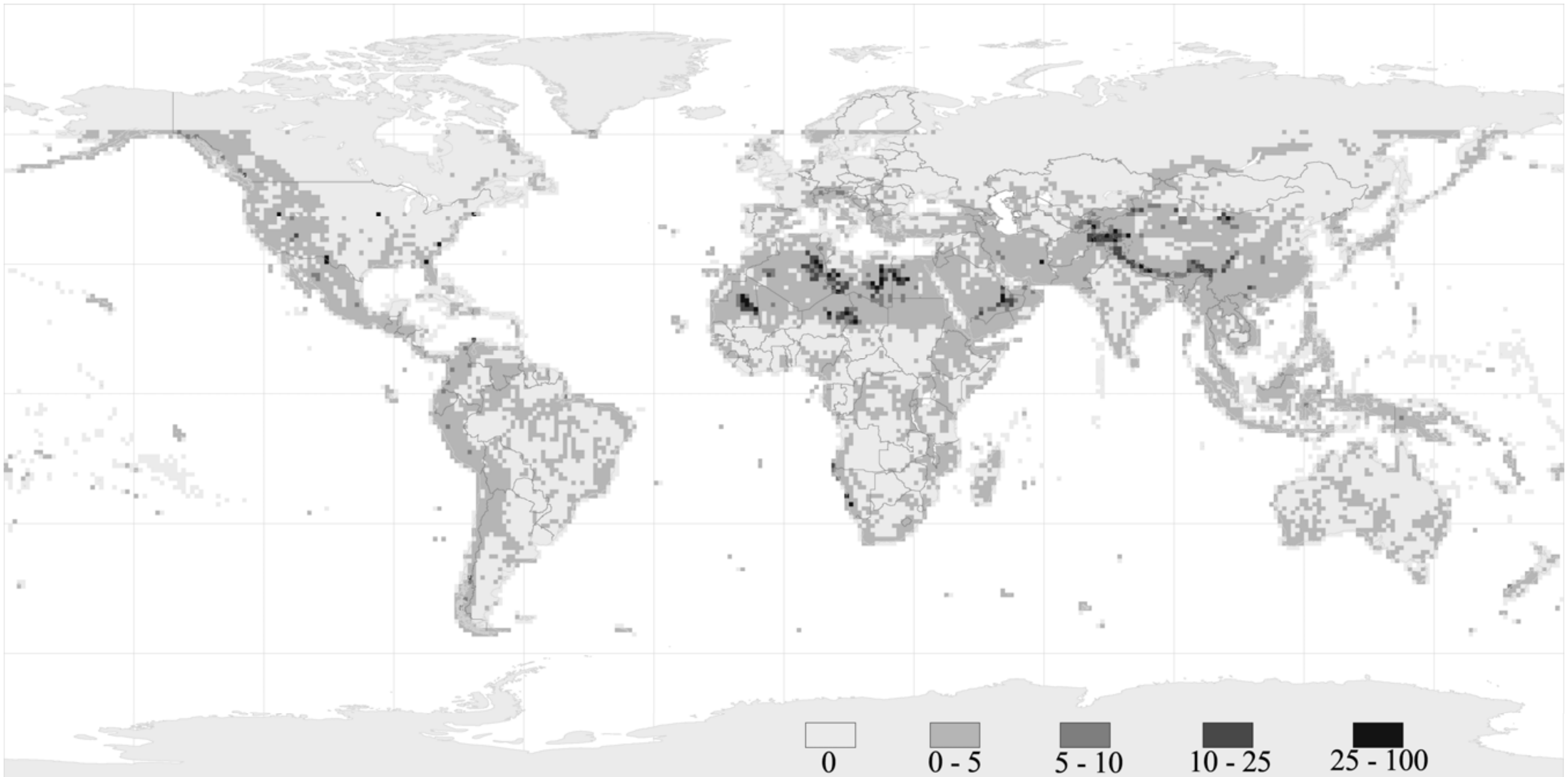

Figure 1

Figure 2

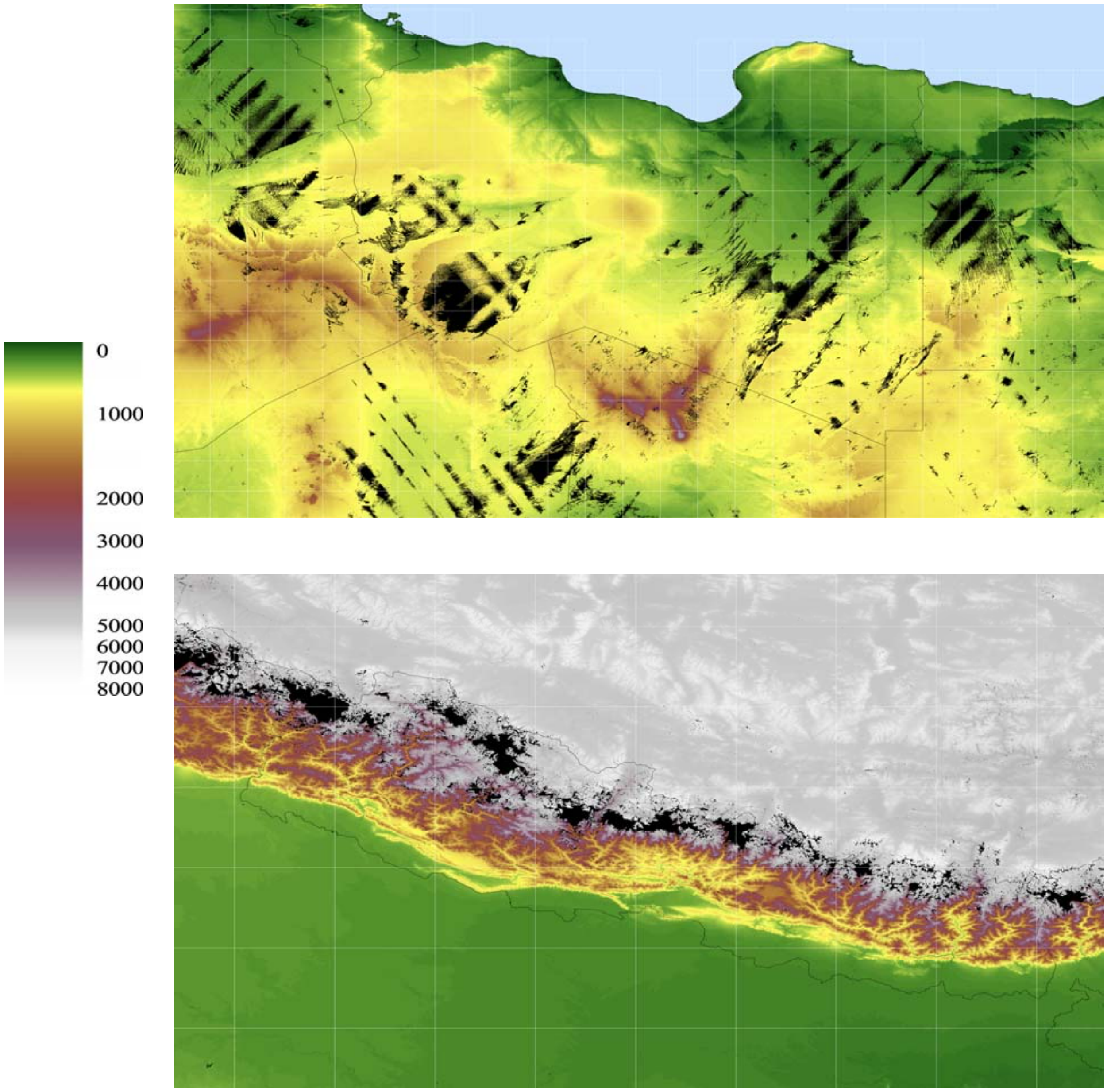

Figure 3

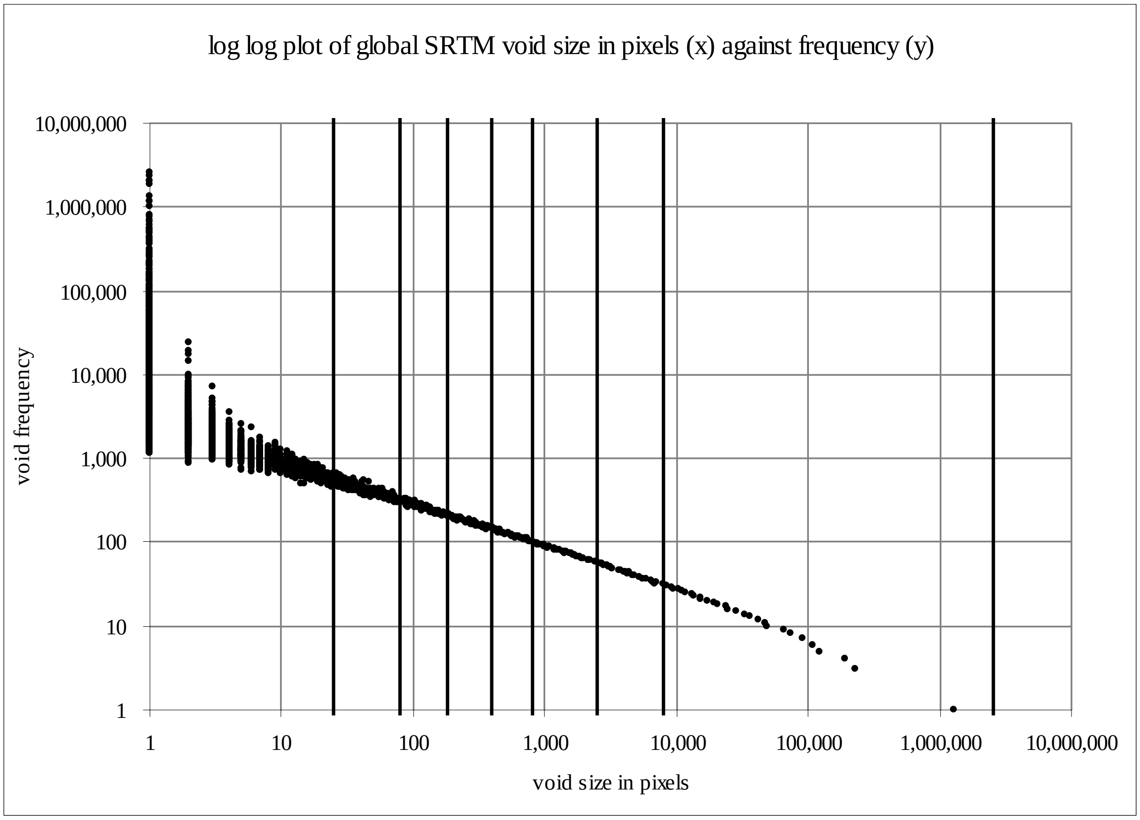
log log plot of global SRTM void size in pixels (x) against frequency (y)
10,000,000
1,000,000
100,000
10,000
1,000
100
10
1
void frequency
1
10
100
1,000
10,000
100,000
1,000,000
10,000,000
void size in pixels

Figure 4

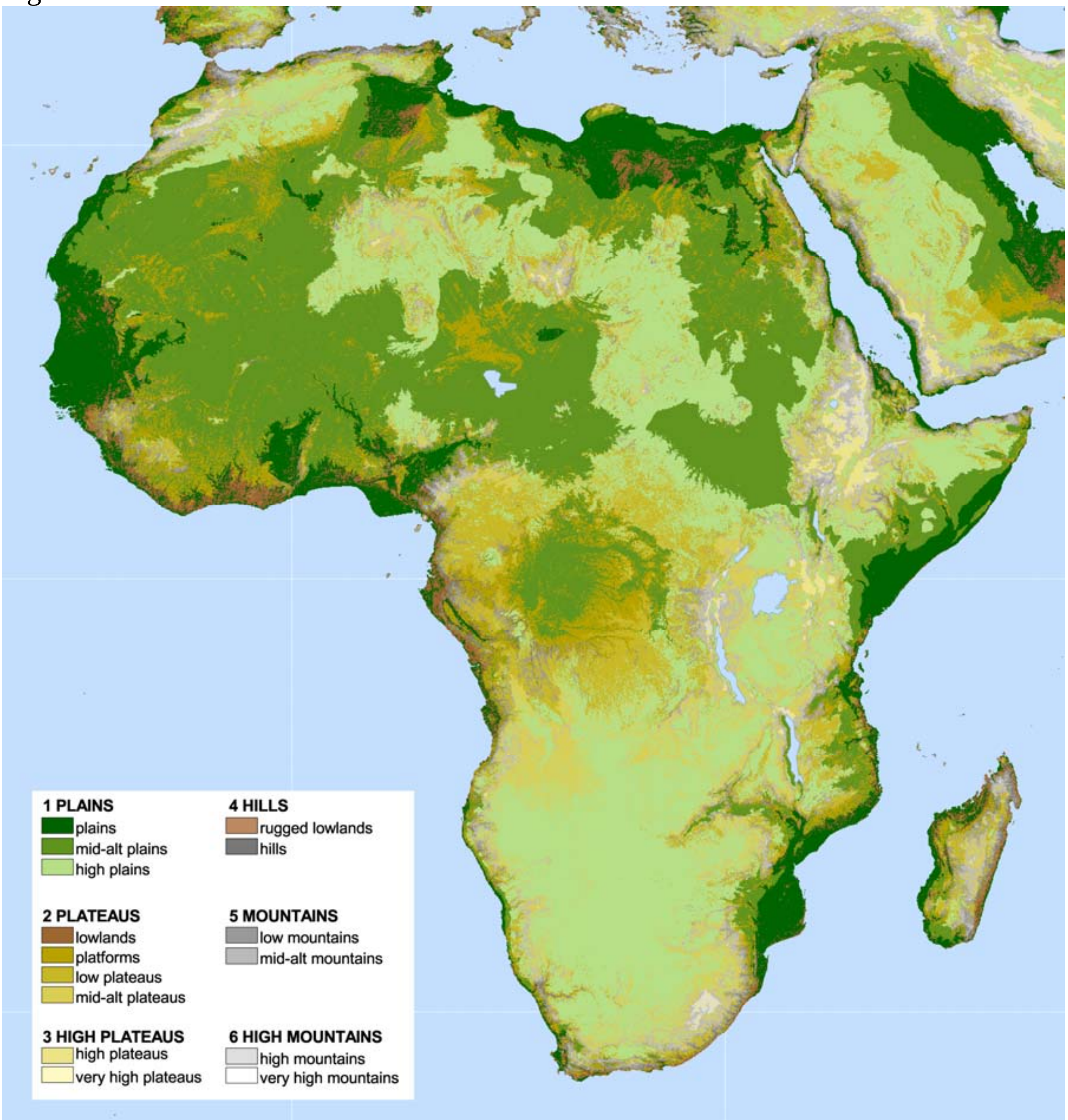
1 PLAINS
plains
mid-alt plains
high plains
2 PLATEAUS
lowlands
platforms
low plateaus
mid-alt plateaus
3 HIGH PLATEAUS
high plateaus
very high plateaus
4 HILLS
rugged lowlands
hills
5 MOUNTAINS
low mountains
mid-alt mountains
6 HIGH MOUNTAINS
high mountains
very high mountains

Figure 5

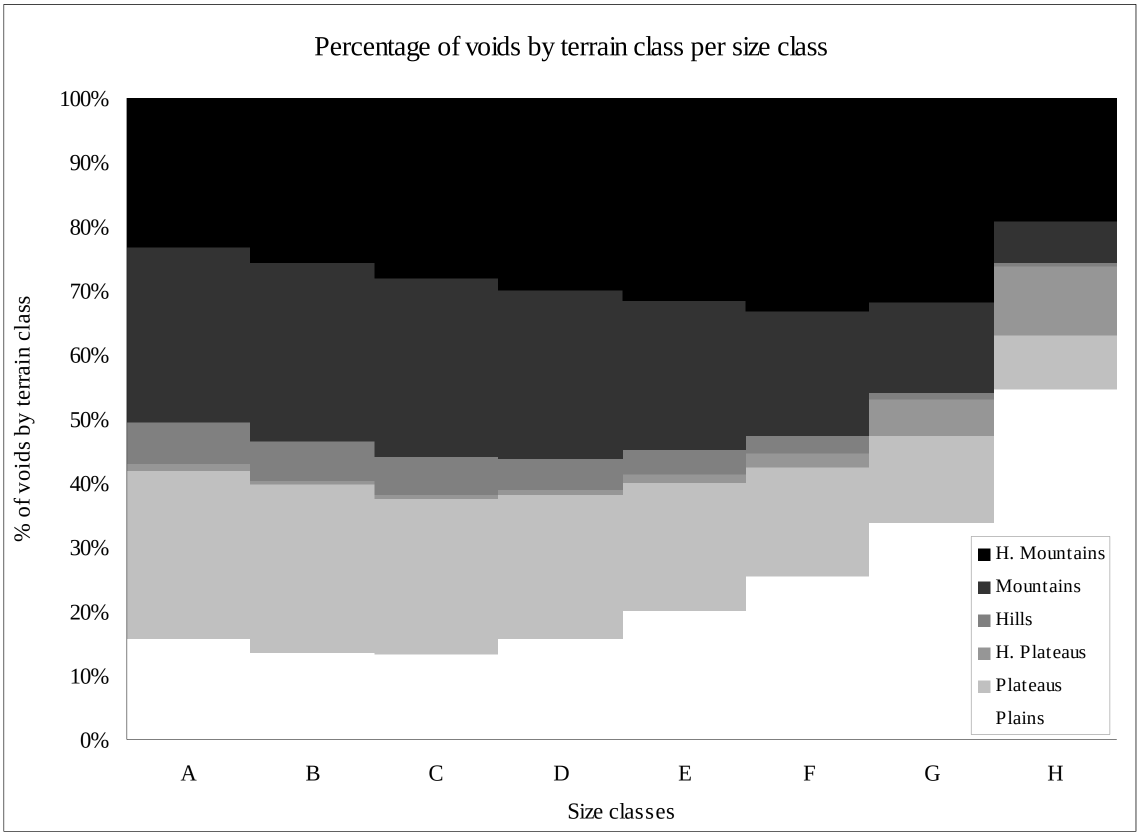

Percentage of voids by terrain class per size class
100%
90%
80%
70%
60%
50%
40%
30%
20%
10%
0%
% of voids by terrain class
A
B
C
D
E
F
G
H
Size classes
H. Mountains
Mountains
Hills
H. Plateaus
Plateaus
Plains

Figure 6

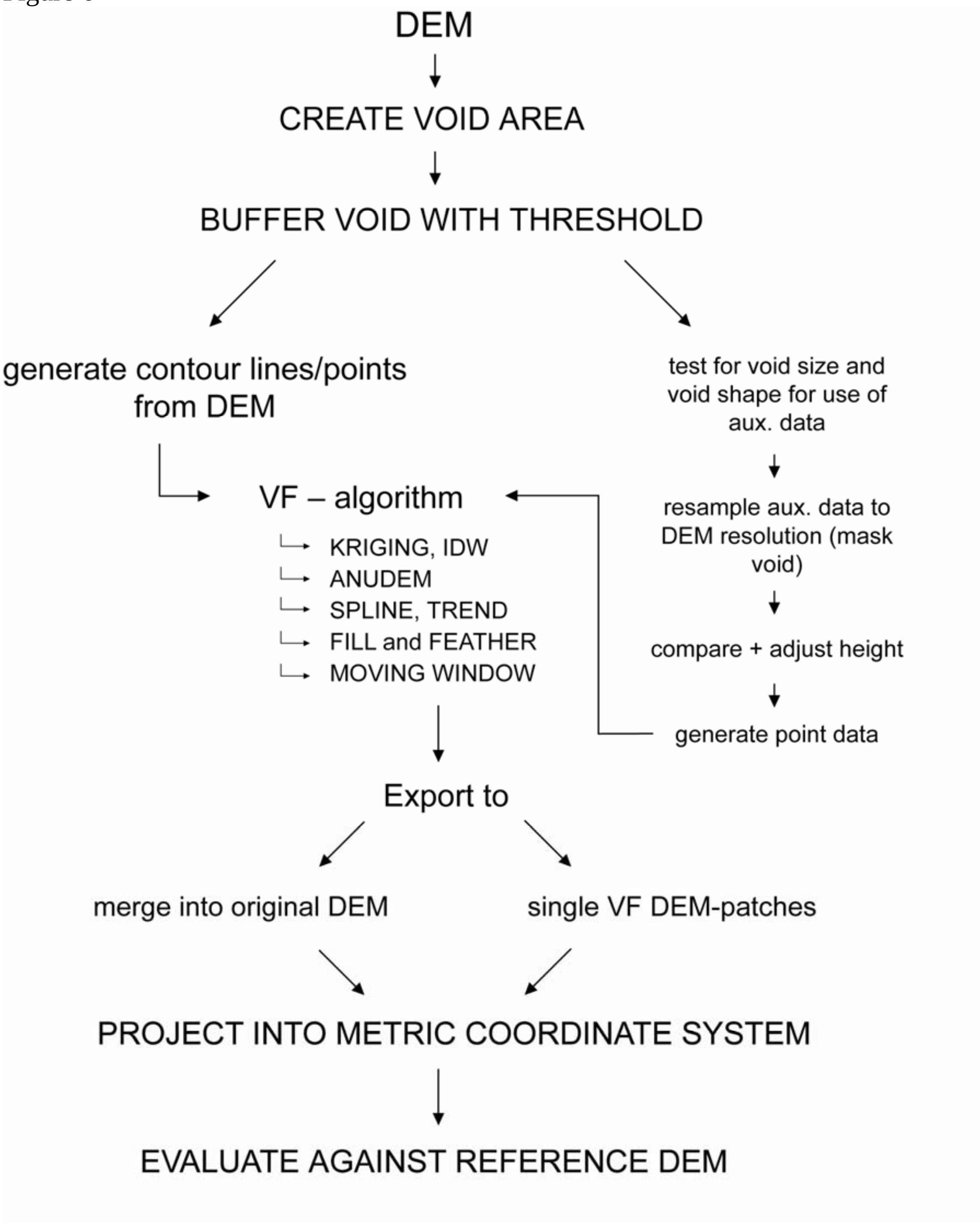
DEM
CREATE VOID AREA
BUFFER VOID WITH THRESHOLD
generate contour lines/points from DEM
test for void size and void shape for use of aux. data
resample aux. data to DEM resolution (mask void)
compare + adjust height
generate point data
VF – algorithm
KRIGING, IDW
ANUDEM
SPLINE, TREND
FILL and FEATHER
MOVING WINDOW
Export to
merge into original DEM
single VF DEM-patches
PROJECT INTO METRIC COORDINATE SYSTEM
EVALUATE AGAINST REFERENCE DEM

Figure 7